Severe Plastic Deformation of Difficult-to-Deform Materials at Near-Ambient Temperatures

M. RAVI SHANKAR, R. VERMA, B.C. RAO, S. CHANDRASEKAR, W.D. COMPTON, A.H. KING, and K.P. TRUMBLE

Plane-strain machining can be used to impart large plastic strains in alloys that are difficult to deform by other severe plastic deformation (SPD) processes. By cutting at low speeds, the heating caused by friction with the tool can be reduced to insignificant levels. The utility of this approach for characterizing microstructure development in SPD is demonstrated using a variety of commercial alloys that exhibit different deformation behaviors and strengthening mechanisms, including CP-titanium, aluminum alloy 6061-T6, nickel-base superalloy IN-718, and pearlitic plain-carbon steel.

DOI: 10.1007/s11661-007-9257-8
© The Minerals, Metals & Materials Society and ASM International 2007

I. INTRODUCTION

NANOSTRUCTURED materials are potentially useful for structural applications because of their significantly improved strength as compared with microcrystalline materials. A major limitation on the widespread use of nanostructured materials is the difficulty in producing fully dense samples composed entirely of a nanoscale microstructure. Severe plastic deformation offers an attractive route for the manufacture of bulk nanomaterials. In pioneering investigations, the effects of large deformation strains on microstructures were studied by Embury and Fisher[1] and Langford and Cohen,[2] who used repeated wire drawing. More recently, the development of severe plastic deformation (SPD) methods, such as equal channel angular pressing (ECAP) and high pressure torsion (HPT), has enabled the systematic study of large-strain deformation and associated microstructure refinement.[3–5] A variety of soft to moderately hard materials have been produced in bulk form with ultra-fine-grained (UFG) and nanocrystalline microstructures using these SPD methods. However, tooling difficulties have usually precluded SPD for difficult-to-deform materials using these methods without some preheating above ambient levels. We discovered an alternative SPD route for imposing large strains at near-ambient temperatures in a single pass of deformation; this route uses chip formation in plane-strain machining.[6]

M. RAVI SHANKAR, Assistant Professor, is with the Department of Industrial Engineering, University of Pittsburgh, Pittsburgh, PA 15261. Contact e-mail: chandy@purdue.edu R. VERMA, Graduate Student, B.C. RAO, Postdoctoral Fellow, S. CHANDRASEKAR, Professor, and W.D. COMPTON, Lillian M. Gilbreth Distinguished Professor Emeritus, Center for Materials Processing and Tribology, School of Industrial Engineering, and A.H. KING, Professor and Head, and K.P. TRUMBLE, Professor, School of Materials Engineering, are with Purdue University, West Lafayette, IN 47907.

This article is based on a presentation made in the symposium entitled "Ultrafine-Grained Materials: from Basics to Application," which occurred September 25–27, 2006 in Kloster Irsee, Germany.

Article published online August 1, 2007.

After a brief metallographic description of microstructure evolution in machining, we demonstrate controlled SPD of difficult-to-deform materials, such as Ti, Al 6061-T6, INCONEL-718,* and pearlitic steels, using plane-strain machining.

*INCONEL-718 and IN-718 are trademarks of INCO Alloys International, Huntington, WV.

II. BACKGROUND

A. *Deformation in Machining*

Severe plastic deformation is a result of chip formation in simple plane-strain (two-dimensional (2-D)) machining, as illustrated in Figure 1, where a sharp, wedge-shaped tool removes a preset depth of material (a_o) by moving in a direction perpendicular to its cutting edge. Deformation occurs by shear concentrated in a narrow zone, often idealized as a shear plane. The geometry of the deformation zone and shear strain in this shear plan model are determined by the shear angle (ϕ) and the rake angle (α). The average shear strain (γ) imposed in the chip is given by[7]

$$\gamma = \frac{\cos\ (\alpha)}{\sin\ (\phi)\cos\ (\phi - \alpha)} \qquad [1]$$

where ϕ is calculated from a measurement of a_o (undeformed chip thickness) and a_c (deformed chip thickness) as

$$\tan\ (\phi) = \frac{\frac{a_o}{a_c}\ \cos\ (\alpha)}{1 - \frac{a_o}{a_c}\ \sin\ (\alpha)} \qquad [2]$$

The principal machining variables controlling the deformation are a_o, α, and the cutting velocity. As suggested by Eq. [1], the shear strain (γ) can be varied by

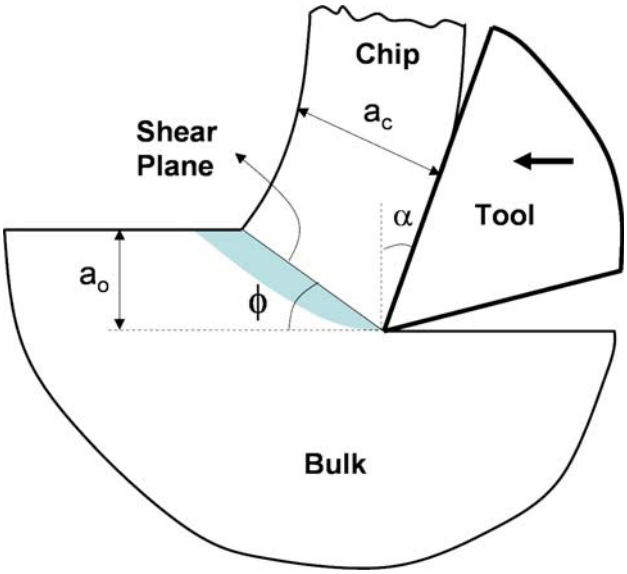

Fig. 1—Schematic of chip formation in plane-strain machining. The shaded zone highlights a fan-shaped deformation region that extends ahead of the tool. The deformation zone is often idealized as a shear plane.

varying the undeformed chip thickness and rake angle, and the strain rate is proportional to the cutting velocity. It is a common misconception that significant heating is inherent in such a machining process. By cutting at low velocities, however, the temperature rise can be easily kept below ~100 °C.

This model of the deformation zone is based on the assumption that all the strain is localized to a plane, and thus the strain essentially represents an upper bound for the deformation during chip formation. Although such an upper bound model provides a simple method for characterizing the deformation strain, a much more accurate characterization can be obtained by *in-situ* measurement of strains using a particle image velocimetry (PIV) technique applied to high-speed images of the deformation process.[8,9] The PIV measurements show the deformation zone to be a fan-shaped region that extends ahead of the cutting tool and the chip into the bulk material. This fan-shaped region is wider in some materials (*e.g.*, titanium), and it is narrower in other material systems (*e.g.*, copper). The largest increments in the deformation strain, however, are still localized and are imposed over a narrow zone that is reminiscent of the shear plane. The fan-shaped region extending ahead of this localized zone, even in materials where it is wide, contributes relatively little to the overall deformation strain in chip formation.[8]

B. *Microstructure Refinement during Machining*

The micromechanics of deformation during the process of chip formation in 2-D machining have been studied using two experimental approaches. First, the classical approach, which involved the observation of slip bands on prepolished surfaces—in this case of pure copper—has provided a preliminary characterization of the extent of deformation in the work piece ahead of the cutting tool.[10] Second, transmission electron microscopy (TEM) was used to observe the dislocation structures in the deformation zone and the concomitant nanostructuring in a more difficult-to-deform material—Al 6061-T6.

C. *Slip-Band Observations in Copper*

In order to study slip band formation in the incipient stage of machining, a 2-mm-thick plate of OFHC copper was first mechanically polished, starting with a series of diamond pastes, and finishing with colloidal silica. The plate sample was then electropolished with a solution of H_3PO_4 in H_2O to relieve the deformation effects caused by the mechanical polishing and to improve further the surface finish. Following this surface preparation, the plate was machined in a single pass with a zero-rake angle high-speed steel (HSS) tool to create a partially detached chip specimen with a plastic shear strain of ~7, as shown in Figure 2. The polished surface was analyzed for slip bands.

Slip-band features were observed on this surface of the work piece ahead of the cutting tool and underneath the partially detached chip (Figure 2). At location (a), furthest from the chip, the slip-band pattern is characterized by a single set of parallel lines. This is indicative of activation of a single slip system in a region that experiences small plastic strains. Closer to the chip, at (b), a mesh of intersecting slip bands is observed, which is indicative of higher levels of strain and activation of multiple slip systems. With further progression toward the chip, (b) to (c) in Figure 2, this mesh pattern becomes increasingly fine until, at a location (d) that is close to the chip, this pattern is so fine that it can be resolved effectively only in a scanning electron microscope (SEM). Although it may not be possible to elucidate the cellular dislocation structures simply from such surface observations of slip bands, it is feasible to delineate the progressive nature of microstructure refinement that occurs during the chip formation. Of course, these observations are limited to regions in which the plastic strains are small enough that the surface is still flat and sufficiently smooth to characterize the slip bands. It is apparent from Figure 2 that in the severely strained chip, the surface is rough, making similar observations of slip bands not only difficult, but also potentially misleading. In these regions, The use of TEM provides a much more effective characterization technique, as demonstrated in Section D.

D. *Dislocation Substructure Development in Chip Formation in Al 6061-T6*

As before, a partially detached chip sample was produced from a 1.6-mm-thick plate of Al 6061-T6 (Figure 3). By using a wedge-polishing technique followed by ion milling for a short duration, an electron transparent sample encompassing the deformation zone was produced. Details of this sample preparation are described elsewhere.[11] In contrast to the slip band observations, TEM characterization offers much more

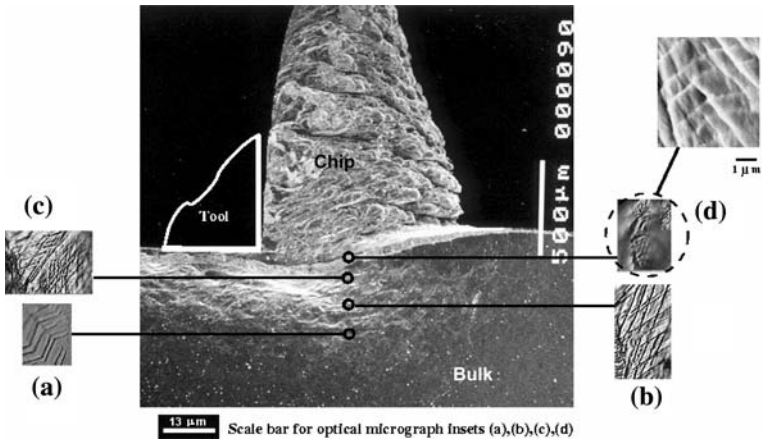

Fig. 2—Evolution of slip-band pattern in deformation zone in plane-strain machining of OFHC copper. The chip is shown in an incipient stage of formation. The area farthest from the deformation zone in inset (a) is characterized by planar slip on a single slip system. Closer to the fully deformed chip, from (*a*) to (*d*), the slip-band pattern becomes finer with activation of multiple slip systems, consistent with the larger strains in these areas.

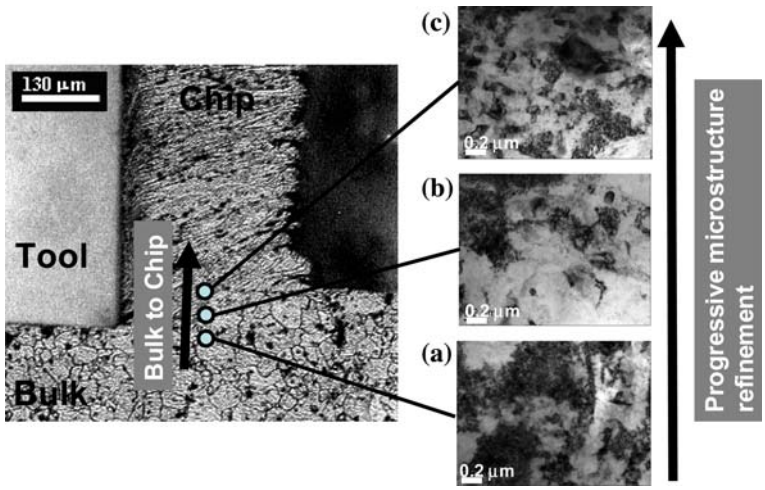

Fig. 3—Structure evolution under SPD of a difficult-to-deform material—Al 6061-T6 (peak-aged). Note the progressive refinement of microstructure in transiting from the bulk to the chip in insets (*a*) through (*c*), as shown by TEM.

direct insight into the microstructure refinement process in the deformation zone. Furthermore, dislocation structures in severely strained regions of the deformation zone can be directly studied.

Figure 3(a) shows a TEM image of a region of the bulk that adjoins the entrance to the deformation zone. The microstructure is composed essentially of large dislocation bundles and carpets. With increasing deformation, the dislocation structures become increasingly refined, and subgrain structures begin to evolve. Approximately midway through the deformation zone, the microstructure consists of a mixture of extended carpets and dislocation bundles, and some subgrain structures, as shown in Figure 3(b). With further deformation, and into the chip, the microstructure is composed entirely of high-misorientation subgrain structures.[11] It was also shown in a related study that, although microstructure refinement is gradual across the deformation zone, the transition of the dislocation structure from a low-misorientation wall to highly-misoriented subgrain structures is rapid and is spatially localized to a small portion of the deformation zone.[11] This rapid transition within a localized region of the deformation zone has also been observed in SPD of Ti by machining, wherein direct measurement of the deformation showed this local region to be characterized by high intensity of strain.[8]

III. DIFFICULT-TO-DEFORM ALLOYS

Building on the emerging evidence for controlled SPD by machining, a series of plane-strain machining experiments was performed to explore SPD of materials of high strength or limited ductility (difficult-to-deform materials). The machining speed was kept sufficiently low (0.6 to 20 m/min) to ensure minimal temperature rise in the deformation zone during chip formation. The

unique nature of the machining process, wherein a significant component of hydrostatic pressure prevails in the deformation zone, permits SPD of even difficult-to-deform materials at near-ambient temperature through the appropriate choice of machining parameters. The remainder of this article demonstrates the described technique on commercially pure (CP)-titanium, INCONEL 718, and pearlitic 1080 steel.

IV. EXPERIMENTAL

For bulk CP-Ti with a Vickers hardness of ~144 kg/mm^2, and a mean grain size of ~60 μm, a HSS tool with a rake angle of +20 deg was used to impose a shear strain of ~3.2 in the chip (estimated using Eqs. [1] and [2]). The machining was performed on a custom-built linear machining device to ensure plane-strain (2-D) conditions. A partially formed chip specimen was created and was metallographically prepared to reveal the bulk microstructure and the resulting SPD microstructures (Figure 4). Chips were also created under identical machining conditions for TEM observation. For this purpose, chips were ground to a thickness of ~100 μm by abrasive polishing, and 3-mm-diameter disks were punched out and thinned to electron transparency by electrolytic jet-thinning (Struers Tenupol-5, Struers, Denmark) using a solution of 60 pct methanol, 35 pct butanol, and 5 pct perchloric acid at –30 °C and 40 V.

INCONEL 718 (grain size ~50 μm and Vickers hardness ~300 kg/mm^2) in a solution-treated condition was similarly subjected to SPD, this time using a commercial ceramic tool with rake angle of –20 deg, resulting in chips with a shear strain of ~6. The much higher strength of INCONEL 718 precluded machining on the linear machining device; instead the chips were created by plane-strain machining of a cylinder of diameter ~150 mm on a lathe.[6,7] The hardness of the chips was measured using Vickers indentation. Thermal stability of the chips produced was characterized by heat treating them at temperatures in the range of 500 °C to 750 °C for different lengths of time. Microstructure of the chips was analyzed by TEM. The specimen preparation procedure followed that for Ti, except that the electrolytic-jet thinning was performed using a solution of 25 pct HNO_3 and 75 pct CH_3OH. The CP-Ti and IN-718 chip samples were examined in a JEOL** 2000FX TEM, operating at 200 kV to characterize the grain size and dislocation structures following the SPD.

**JEOL is a trademark of Japan Electron Optics Ltd., Tokyo.

The SPD of bulk 1080 steel with a coarse pearlite microstructure was performed to analyze the effects of large-strain deformation of a lamellar two-phase microstructure. The coarse pearlite microstructure was created by heat treating a 25.4-mm-diameter bar of 1080 steel at 800 °C for 2 hours, followed by controlled furnace cooling to 650 °C at a rate of 28 °C per hour over ~5.5 hours. The bar was then allowed to cool to room temperature inside the furnace. The resulting coarse pearlite had an interlamellar spacing of ~716 nm and an initial Vickers hardness of 238 kg/mm^2. This material was subjected to a strain of ~3.8 by plane-strain machining on the lathe with a +5 deg-rake angle HSS tool. The pearlitic microstructure in the bulk and chip samples was revealed by etching with a solution of 4 g of picric acid in 100 mL of ethanol. A combination of atomic force microscopy (AFM) and optical microscopy was used to analyze the pearlite microstructure in the chip and bulk samples. Hardness values in different regions of the pearlite were analyzed using nanoindentation with a Berkovitz indenter at 250-nm depth.

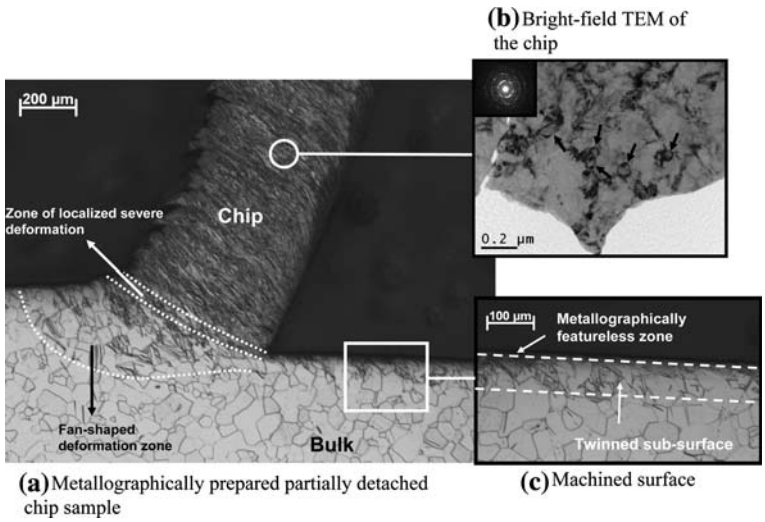

Fig. 4—Microstructure refinement and formation of UFG Ti by chip formation. Note the mechanical twinning at the smaller levels of strain in the fan-shaped deformation zone ahead of the tool and in the subsurface left behind. At the larger levels of strain, metallographically featureless regions are observed; for example, the chip in (*a*) and the machined surface in (*c*). TEM micrograph of inset (*b*) confirms the nanostructured nature of this metallographically featureless zone.

V. RESULTS AND DISCUSSION

A. *CP-Titanium*

Figure 4(a) shows an optical micrograph of a partially detached CP-Ti chip sample. Destruction of microstructural features of the bulk is clearly evident as the material undergoes SPD in a fan-shaped deformation zone to a metallographically featureless chip. The chip is composed of ~100-nm-sized grains, as shown in the TEM micrograph of Figure 4(b). Concomitant with this microstructure refinement, the hardness value increased from ~144 kg/mm^2 in the bulk to ~230 kg/mm^2 in the chip. In contrast to the Al 6061-T6 (Figure 3), the transition in the microstructure from the bulk to the chip is more gradual in the CP-Ti, and the transition occurs over two distinguishable portions of the deformation zone. The first, a fan-shaped deformation zone, is associated with somewhat smaller values of shear strain (<0.4) as revealed by particle image velocimetry (PIV)[8] and retention of metallographic features inherited from the bulk together with a preponderance of deformation twins (Figure 4(a)). These twin orientations have been characterized using EBSD and will be the subject of a forthcoming publication.

The relatively small level of deformation strain in the fan-shaped deformation zone is followed by a zone of localized severe deformation (Figure 4(a)). Here, all the metallographic features inherited from the bulk are destroyed, resulting in a featureless chip when observed under the optical microscope. The multiplicity of the deformation modes and the levels of deformation strains encountered during chip formation also manifest themselves in the metallographic characteristics of the residual machined surface (Figure 4(c)). The region closest to the surface is inherited from the zone of localized severe deformation, and further into the subsurface a region of extensive twinning is observed. This region, inherited from the fan-shaped deformation zone associated with smaller levels of strain, is characterized by a proliferation of deformation twins and a preservation of many of the bulk microstructural features. Through *in-situ* observations using a PIV technique and high-speed microphotography, the levels of strain and strain rate in the various zones of deformation have been measured and correlated with the microstructure features, such as twins and nanostructures in the chip and work surface.[8]

B. *INCONEL 718*

Figure 5 shows a TEM micrograph of an INCONEL 718 chip with grains typically ~100 nm in size. The selected area diffraction (SAD) pattern in Figure 5 also indicates the occurrence of significantly misoriented grain and subgrain structures, as evidenced by the ringlike pattern around the central spot. When this severely deformed chip sample is subjected to heat treatment at 600 °C in air, very rapid aging is observed, which is likely associated with accelerated precipitation kinetics in the nanostructured chip. The chip material reaches a peak hardness of ~630 kg/mm^2, after only 6 hours at 600 °C, from an initial hardness of ~550 kg/mm^2 after the SPD.

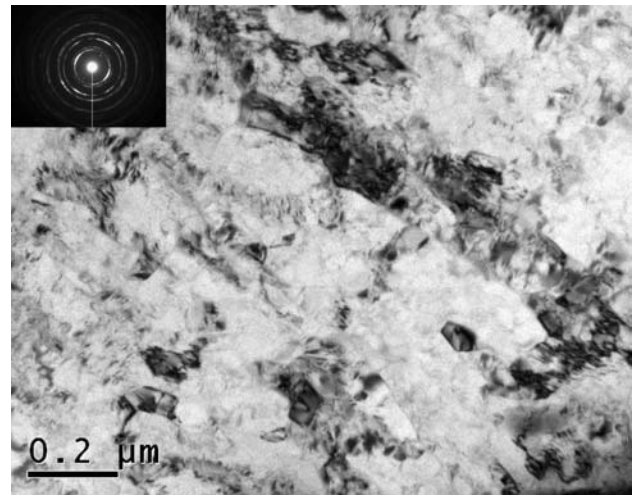

Fig. 5—UFG microstructure in solution-treated INCONEL 718 after SPD to a shear strain of 6 by machining with a –20 deg rake angle tool.

In contrast, INCONEL 718 in the bulk microcrystalline state is usually characterized by sluggish precipitation kinetics that necessitate extended thermal processing to achieve peak material strength.[12] This observation of rapid aging in the INCONEL 718 chips is similar to that observed in Al 6061, wherein chips cut from solution-treated 6061 aged more rapidly and at lower aging temperatures to reach a peak strength significantly greater than that of the undeformed bulk material in a microcrystalline state. These observations suggest the possibility of chips that are machined from solution-treated bulk material being dynamically aged during a high-temperature consolidation process, thereby enabling the manufacture of fully dense, bulk nanostructured materials.

C. *Pearlitic 1080 Steel*

The SPD of 1080 steel with a coarse pearlite microstructure shows a deformation mechanism that is nonuniform as compared with that observed with single-phase CP-Ti or solution-treated INCONEL 718. The initial, undeformed bulk steel microstructure consists of pearlite with an average interlamellar spacing of 720 nm (Figure 6). The Vickers hardness of the bulk material is 238 kg/mm^2. The AFM observations of the chips created with a shear strain of ~3.8 show formation of two distinct pearlitic ensembles. The first ensemble consists of highly collated, dense structures, consisting of parallel cementite lamella. This "refined pearlite," illustrated in Figure 7, has an interlamellar spacing of 520 nm, which is smaller by almost 30 pct than that in the undeformed bulk material. Aligned almost parallel to this refined pearlite are bands of bent and broken pearlitic structures; the "broken pearlite" is also shown in Figure 7. Nanoindentation shows the hardness of the refined pearlite is ~5.2 GPa, whereas that of the broken pearlite is ~4.7 GPa. For comparison, the nanohardness of the undeformed bulk material is ~3 GPa. This clearly

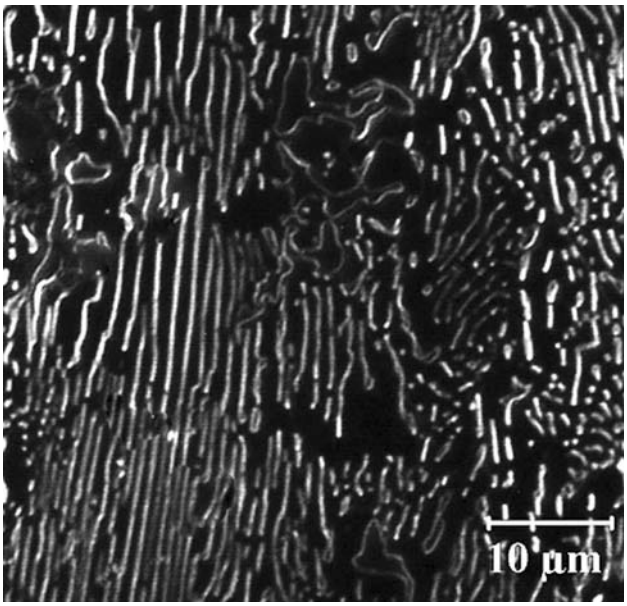

Fig. 6—Optical micrograph of bulk 1080 steel showing a coarse pearlite microstructure.

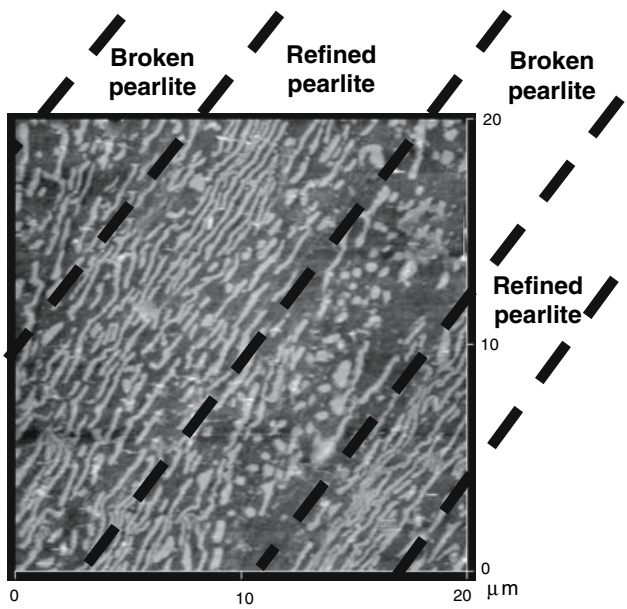

Fig. 7—Microstructure of 1080 steel chip as shown by AFM. Note occurrence of two distinct pearlitic ensembles—refined pearlite and broken pearlite, as a result of the SPD by machining.

illustrates the formation of a mechanically and microstructurally inhomogeneous chip material (~10-μm scale) following SPD of the coarse lamellar structure.

This inhomogeneity in the chip microstructure may be traced to different orientations of the pearlite lamellae in the undeformed bulk material. In different pearlite colonies of the bulk steel, the lamellae are differently oriented, and when they enter the deformation zone (idealized as a plane for the sake of discussion), some are oriented more parallel to the shearing direction than

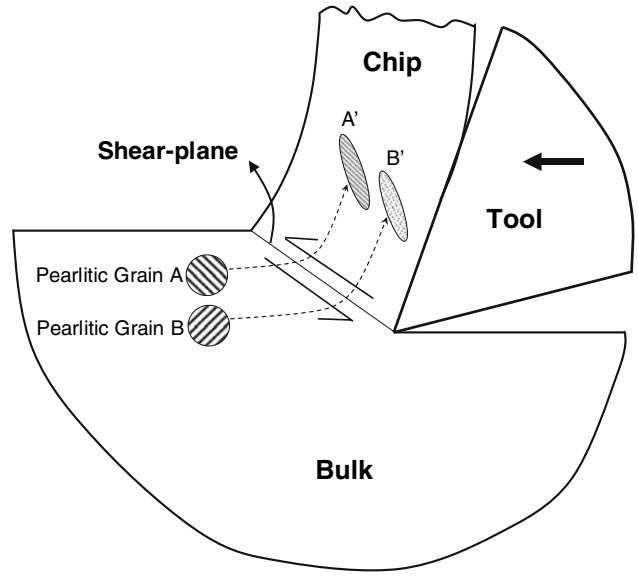

Fig. 8—A possible mechanism for development of the nonuniform pearlitic microstructure in the chips. Pearlite colony A, with lamellae oriented approximately parallel to the shear direction, undergoes refinement to pearlite A′, whereas pearlite colony B, oriented transverse to the shear plane, is broken up during the SPD resulting pearlite B′.

others. This aspect is illustrated schematically in Figure 8, wherein colony A, which is more favorably oriented for deformation at the shear plane, undergoes SPD to result in a refined pearlitic structure (A′) in the chip. On the other hand, colony B, which is less favorably oriented for deformation with respect to the shear direction, is likely to undergo severe bending and fragmentation resulting in the broken pearlite (B′) in the chip. Thus, the inhomogeneity of the chip microstructure is a consequence of the varying orientations of lamellae in the bulk material with respect to the direction of shear in the deformation zone.

The ability to perform controlled SPD of steels to large strains in a single pass opens up exciting possibilities for various microstructure-related studies, such as break-up or dissolution of cementite, creation of ultrafine pearlitic microstructures, and extensions of Embury and Fisher's pioneering work.[1]

VI. SUMMARY

Severe plastic deformation of difficult-to-deform materials—Al 6061-T6, CP-Ti, solution-treated INCONEL 718, and pearlitic 1080 steel—has been demonstrated at near-ambient temperature using machining. For materials with a uniform initial microstructure, such as the CP-Ti and INCONEL 718, the SPD by machining results in a nanostructured chip with grain sizes typically ~100 nm. Furthermore, in the CP-Ti, metallography across the deformation zone showed mechanical twinning in the early stages of deformation (shear strain $<$ 0.4) before entering the zone of intense shear. With increasing deformation, all metallographic features

inherited from the bulk material are destroyed, and a nanostructured chip material typically results. When the starting bulk material has a nonuniform microstructure, such as the pearlitic 1080 steel with a coarse lamellar microstructure, the chip produced by SPD is composed of two distinct, alternating pearlitic ensembles—"refined pearlite" and "broken pearlite." Such inhomogeneity may be traced to the differing orientations of the pearlite in the polycrystalline, undeformed bulk material with respect to the direction of shear in the deformation zone. In summary, the evidence presented reinforces the efficacy of machining as a versatile, controlled single-pass method for imposing large plastic strains, even in difficult-to-deform materials at near-ambient temperatures.

ACKNOWLEDGMENTS

The authors acknowledge the United States Department of Energy (Grant No. 4000031768 *via* UT–Battelle, Dr. Ray Johnson, Program Manager), Oak Ridge National Laboratory, the NSF (Grant No. DMI-0500216), and Sandia National Laboratory (Dr. Pin Yang, Technical Program Manager) for supporting this work.

REFERENCES

1. J.D. Embury and R.M. Fisher: *Acta Metall.*, 1966, vol. 14, pp. 147–59.
2. G. Langford and M. Cohen: *Trans. ASM*, 1969, vol. 62, pp. 623–38.
3. V.M. Segal, V.I. Reznikov, A.E. Drobyshevskiy, and V. Kopylov: *Russ. Metall.*, 1981, vol. 1, pp. 99–105.
4. M. Furukawa, Z. Horita, M. Nemoto, and T.G. Langdon: *Mater. Sci. Eng., A*, 2002, vol. 324, pp. 82–89.
5. R.Z. Valiev, R.K. Islamgaliev, and I.V. Alexandrov: *Progr. Mater. Sci.*, 2000, vol. 45, pp. 103–89.
6. T.L. Brown, S. Swaminathan, S. Chandrasekar, W.D. Compton, A.H. King, and K.P. Trumble: *J. Mater. Res.*, 2002, vol. 17 (10), pp. 2484–88.
7. M.C. Shaw: *Metal Cutting Principles*, Clarendon, Oxford, United Kingdom, 1984.
8. M. Ravi Shankar, B.C. Rao, S. Lee, S. Chandrasekar, A.H. King, and W.D. Compton: *Acta Mater.*, 2006, vol. 54 (14), pp. 3691–700.
9. S. Lee, J. Hwang, M. Ravi Shankar, S. Chandrasekar, and W.D. Compton: *Metall. Mater. Trans. A*, 2006, vol. 37A, pp. 1633–43.
10. J. Friedel: *Dislocations*, Pergamon, London, 1964.
11. M. Ravi Shankar, S. Chandrasekar, W.D. Compton, and A.H. King: *Mater. Sci. Eng., A*, 2005, vols. 410–411, pp. 364–68.
12. S.J. Hong, W.P. Chen, and T.W. Wang: *Metall. Mater. Trans., A*, 2001, vol. 32A, pp. 1887–901.